STRUCTURE, MEMORY AND SPLITTING OF TURBULENT SPOTS IN TRANSITIONAL PIPE FLOW WITHOUT AXIALLY PERIODIC BOUNDARY CONDITION

Xiaohua Wu

Royal Military College of Canada

Parviz Moin

Center for Turbulence Research, Stanford University

Ronald J. Adrian

Arizona State University, USA

ABSTRACT

We begin our investigation by studying scalar flash, turbulent spot and transition statistics in a 500 radii-long pipe configuration at Reynolds number 6500, based on the bulk velocity and the pipe diameter. During the late stage of transition, second-order statistics such as the rate of dissipation of turbulent kinetic energy exhibit substantial overshoot, which is accounted for by the observed stronger mid-to-high frequency content in the spectra of the rate of dissipation. Transitional turbulent spots are found to have a dual-type structural composition. The near-wall region consists of primarily reverse hairpin vortices with their head element directing towards the upstream direction and towards the wall. This composition is related to the high-speed streaks arising from the prescribed inlet perturbation. The core region of the spots on the other hand is populated by normal hairpin vortices. Passive scalar injected at the center of the inlet plane develops during transition into what we call the Type-1 flash, which is bounded by non-turbulent region(s) from at least one end, and it is directly associated with the transitional-turbulent spot. Immediately downstream of the high-scalar-value Type-1 flash is a zone with sharply lower scalar value. This results in a segmented scalar field pattern propagating well into the downstream fully turbulent pipe flow, forming what we call the Type-2 scalar flash residing in a turbulent environment. At several hundred radii downstream of transition where the flow is fully-developed and turbulent, the Type-2 scalar flashes serve as carriers of persistent memory of the far upstream transition.

In the second stage of the investigation, we use a 1000 radii long pipe flow to study the splitting of turbulent spots, a feature first discovered by E.R. Lindgren (Arkiv Fysik, **16**, 101-112, 1959a). Reynolds number is 2300. The simulation design asymptotes the idealized scenario in which a blob of turbulence introduced from the inlet develops through fully-developed laminar flow in a very-long smooth pipe. The instantaneous axial velocity along the centerline remains almost exactly as the expected laminar value both upstream and downstream of the migrating turbulent spot packet, which permits simple and accurate capturing of the front and tail positions of the perturbed region. Although the first generation of splitting event occurs in a relatively straightforward manner, the ensuing turbulent spot packet enters an unexpected quasi-cyclic process containing previously unknown sub-processes of parent-child reconnection and re-splitting rather than the anticipated successive generational splitting. Conditional sampling with the aid of the iso-surfaces of swirling strength shows that the frontal zone of a spot travels measurably and constantly faster than its middle section, suggesting that the splitting of pipe turbulent spot is most likely due to a sustained zonal speed difference (streamwise stretching) between the spot's frontal zone and the core. Passive scalar results demonstrate that the zone occupied by the migrating spot packet is only a small subset of the zone impacted by the packet. We are of the opinion that turbulent spot splitting is an interesting feature that is only important for internal transitional flows within a very narrow range of Reynolds number.

INTRODUCTION

In a series of papers on pipe transition experiments, Lindgren systematically studied the transition process using modern optical equipment (Lindgren 1953, 1959a,b,c). Lindgren defined turbulent spot as a near-wall, self-preserving, turbulent-flow patch from which eddies contaminate the nearby quiescent region of the flow. Turbulent flash was also given a different name by Lindgren (1953) as turbulent slug, defined by him as a turbulent spot or spots with a core that fills the entire spanwise/circumferential dimension of the configuration. Based on his experimental visualizations, Lindgren concluded that transition in pipe flow implies the formation of turbulent spots under finite amplitude perturbations, and commented that this understanding was consistent with the boundary layer work of Schubauer & Skramstad (1947) and Schubauer & Klebanoff (1955). Further, Lindgren (1953) pointed out that turbulent spots observed in boundary layer and turbulent flashes or slugs in pipe flow represent one and the same transition process, albeit at different stages of development. Twenty years later, Wygnanski and Champagne (1973) subdivided the slug concept of Lindgren (1953) into puff (spot in low-Reynolds number) and slug (spot in higher Reynolds number). Thus, for generality and consistency with boundary layer study, we prefer the original terminology of turbulent spot in lieu of turbulent flash, turbulent patch, turbulent slug, turbulent puff and turbulent stripe. Many of the experimental photographs of Lindgren (1959a) show that chaotic bentonite suspension patches appear to be present in the downstream fully-developed turbulent pipe flows at $Re = 3740$ and 7640. He only made this observation in passing without giving any further comments. Intuitively one would think like Lindgren that these are related to some large-scale coherent structures in turbulent flow. Are these the turbulent-turbulent spots discovered recently from the inner region of the flat-plate turbulent boundary layer (Wu et al 2017), or are they something else? The turbulent-turbulent spots in Wu et al are inside the inner layer ($y^+ < 100$) of the boundary layer whereas the 'turbulent scalar patch' observed by Lindgren (Figure 1) from fully-developed turbulent flow occupies the entire pipe cross-section. It turns out,

based on the present study, that the chaotic bentonite suspension patches in question, even though they reside in turbulent flow, are most likely scalar patches created due to the far upstream breakdown of the laminar flow. In other words, they are the passive scalar field's memory of the upstream transition.

Examination of the three-dimensional vortex elements of matured turbulent spots in the present study at $Re = 6500$ reveals that the core region is populated by normal hairpin vortices, and the near-wall region is dominated by reverse hairpin vortices. This is a new discovery. The origination of the near-wall reverse hairpin vortices turns out to be associated with high-speed streaks introduced inadvertently from the prescribed inlet condition in both cases. Energy growth rate as a function of axial distance is also evaluated. The overshoot behavior of turbulent statistics during late stage of pipe transition is identified, and the mechanism behind such overshoot is addressed.

An additional new finding out of the first part of our study at $Re = 6500$ is as follows. Scalar flashes were observed to first appear during transition corresponding to the formation of transitional-turbulent spots possessing strong turbulent mixing capacity. These (chaotic) scalar flashes (Type-1) are bounded by laminar flow either from both ends or from at least the upstream side, and their appearance is expected. Interestingly, the scalar flashes are found to propagate in an orderly succession manner well into the full-developed turbulent region. The cross-section integrated instantaneous scalar flow rate exhibits zig-zag pattern. Such scalar flashes residing and propagating in a fully turbulent flow environment are what we call the Type-2 flashes. They serve as the memory carrier of the far upstream transition even at several hundred radii downstream of the laminar flow breakdown location. This discovery affords convincing explanation to the mysterious 'turbulent scalar patch' residing in the fully-turbulent region observed experimentally sixty years ago by Lindgren.

Aside from directly photographing the scalar fields in the pipe flow, Lindgren also collected instantaneous traces from an optic-electronic oscillogram which involved polarized light beam, polarized sheet, and photo-multiplier. The oscillation level of the traces corresponds qualitatively to the local magnitude of turbulent shear stress in his pipe flow. Lindgren (1959a) noted that, at $Re = 2800$, the turbulent spots migrating between his Station IV ($244R$ from the inlet) and Station V ($400R$ from the inlet) have developed a tendency to split into two units. The child spot always develops ahead of the parent spot within the disturbed flow region. He only made this observation in passing without giving any further comments.

In the second stage of our investigation, we perform DNS of turbulent spot splitting using the spatially-developing pipe transition simulation approach. The simulation design asymptotes the idealized situation in which a blob of turbulence introduced from the inlet develops through fully-developed laminar flow in a very-long smooth pipe. Evidence to the successful asymptote is found in that the centerline axial velocity component extracted from DNS remains almost exactly as the expected value $2V$ both upstream and downstream of the migrating packet of turbulent spots. Friction factor results show similar accuracy. See Figure 1. This is in sharp contrast to existing temporal DNS studies on pipe spot splitting. The quantitative accuracy achieved in the present study allows us to easily locate the front and tail positions of the zone impacted by a migrating turbulent spot packet from its ambient laminar flow.

It turns out that although the first generation of splitting event occurs in a relatively straightforward manner, the ensuing turbulent spot packet enters an unexpected quasi-cyclic process containing previously unknown sub-processes of reconnection of all the elements in an entire packet of spots, and re-splitting after reconnection. This is quite different from the simple successive splitting scenario (parent to child to grandchild) envisioned in the literature. Previous work on pipe flow spot splitting often left the impression that splitting is a mysterious characteristic common to all turbulence. Our conditional sampling results on isolated turbulent spots indicate that zonal axial velocity difference (streamwise stretching) on the downstream half of a pipe flow spot may be the root cause for the splitting.

METHOD

The governing equations are the continuity and the Navier-Stokes equations for incompressible flow in cylindrical coordinates. The fractional step method based computer program and the details of the numerical scheme were described by Pierce and Moin (2001, 2004) in their large-eddy simulation of combustion in a co-axial jet combustor. That configuration is degenerated into a spatially developing circular pipe in this work.

For the first DNS, at $Re = 6500$, the pipe length is $500R$, and the computational mesh size is $16384\times200\times512$ in the axial, radial and azimuthal directions, respectively. Time step remains a constant $\Delta t = 0.005R/V$. The inlet base flow has the fully-developed parabolic laminar velocity profile, except for that inside a three-degree narrow numerical wedge. Within the numerical wedge, the exact laminar parabolic velocity profile is replaced by the time-dependent, fully-developed turbulent pipe DNS velocity field at $Re = 5300$ (Wu & Moin 2008), mimicking to some extent the narrow turbulent wake behind a thin splitter plate. A passive scalar (represented by symbol ϕ) is also added through the introduction of numerical dye over the inlet plane in a region very close to the pipe axis ($0 \le r \le 0.05$), similar to the syringe needle injection of dye by Osborne Reynolds. Adiabatic zero-flux boundary condition for the scalar is imposed on the pipe wall. Molecular Prandtl number for the passive scalar is chosen as 1.

For the second DNS, at $Re = 2300$, the pipe length is $1000R$— a factor of four increase compared to that in Wu et al (2015). The computational mesh size is $32768\times200\times256$ in the axial, radial and azimuthal directions, respectively. Time step remains a constant, $\Delta t = 0.01R/V$. The inlet base flow has the fully-developed parabolic laminar velocity profile, except for a short time interval inside a sixty-degree narrow numerical wedge. For $0 \le t \le 20R/V$, within this numerical wedge, the exact laminar parabolic velocity profile is replaced by the time-dependent, fully-developed turbulent pipe DNS velocity field at $Re = 5300$ (Wu 2017). For $t > 20R/V$, the laminar velocity profile is restored inside the wedge. An artificial turbulence spot is thus introduced from the inlet, which is broadly analogous to the way of producing pipe flow turbulent spots at low Reynolds number in previous experimental studies (Nishi et al 2008, Avila et al 2011).

RESULTS

In the first present pipe DNS at $Re = 6500$, second-order turbulence statistics collected in the late transitional region exhibit sharp overshoot compared to the corresponding profiles in the downstream fully-developed turbulent region. Figure 1 shows the radial profiles of normalized rate of viscous dissipation of turbulence kinetic energy $\varepsilon^+ = \varepsilon/({u_\tau}^4/\nu)$ as a function of $(1 - r/R)^+$. In the figure, the results sampled from the fully-developed turbulent region ($z = 225R, 400R$) collapse over those extracted from the auxiliary axially-periodic DNS on fully-developed turbulent pipe flow. Overshoot with reference to these turbulent profiles is displayed distinctively in Figure 1 by the profiles sampled in the late transitional zone ($z = 30R, 82.5R$). Overshoot is observed regardless whether the profiles are normalized by inner or outer variables. Inner variables such as u_τ and $y^+ = (1 - r)^+$ vary with axial distance in pipe flow during transition whereas outer variables V and R are constants. The overshoot of turbulent statistics during late transition may be a distinct feature of internal transitional flows where the Reynolds number is constant with respect to axial distance. For external transitional flows such as the zero-pressure-gradient smooth flat-plate boundary layer (ZPGSFPBL), it is unclear whether such distinct overshoot can be easily identified. As an illustration, Figure 2 shows the local peak value of $u'^2_{x,rms}/U^2_\infty$ as a function of the momentum-thickness Reynolds number Re_θ in ZPGSFPBL. Note here the subscript x refers to the boundary layer streamwise direction along which Re_θ grows (in experiments and in spatially-developing DNS). In the figure, the DNS results were extracted from the ZPGSFPBL of Wu et al (2017), which develops from laminar through bypass transition (in the narrow sense) to a fully turbulent state. Also included in the figure are the low Reynolds number turbulent ZPGSFPBL experimental data of Purtell et al (1981), Erm & Joubert (1991). By comparing the levels reached in DNS during the stage of late transition and the experimental data acquired from turbulent ZPGSFPBL at similar range of low Re_θ, one can make the observation that there might be a plausible overshoot. The degree of the potential overshoot, if it indeed exists, is nevertheless quite minor with respect to the observed distinct overshoot during pipe transition shown in Figure 1.

Figure 3 shows the iso-surfaces of $\lambda_{ci} = 1.5$ revealing a matured transitional-turbulent spot. At this particular instant the spot has expanded across over the entire 360^o circumferential direction, but they have not merged into the downstream continuous turbulent region yet. In the original definition of Lindgren (1959a), this turbulent spot would be considered as a 'turbulent slug'. It is evident from the particular viewing angle of Figure 3 that the near-wall region of the transitional-turbulent spot composes primarily of reverse hairpin vortices inclined towards the upstream direction with head element pointing towards the wall. In a ZPGSFPBL, the normal hairpin vortices are inclined towards the downstream direction with their head elements pointing towards away from the wall. Such near-wall spot composition is general for the present pipe transitional flow, and is not unique to this particular transitional-turbulent spot in Figure 3. The viewing angle for Figure 3 is such that the pipe core region is blocked by the dense near-wall reverse hairpin vortices. We also found that the core region of the turbulent spot consists of mostly normal hairpin vortices, suggesting that the pipe transitional turbulent spots can have an interesting dual-mode structural composition.

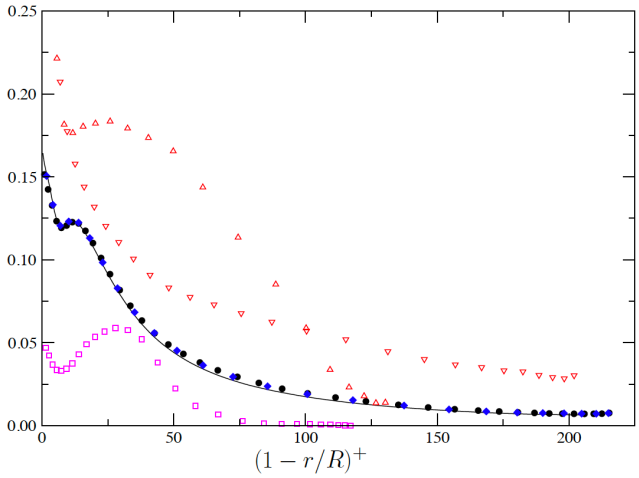

Figure 1. Rate of dissipation of turbulence kinetic energy ε^+ at $Re = 6500$. Solid line: present auxiliary DNS with the conventional axially-periodic boundary condition on a 30R-long fully-developed turbulent pipe flow. Symbols: the present spatially-developing simulation. Circle $z = 400R$; diamond $z = 225R$; nabla $z = 82.5R$; triangle $z = 30R$; box $z = 15R$. Notice that the two profiles in the late transitional zone overshoot the fully-developed turbulent profiles.

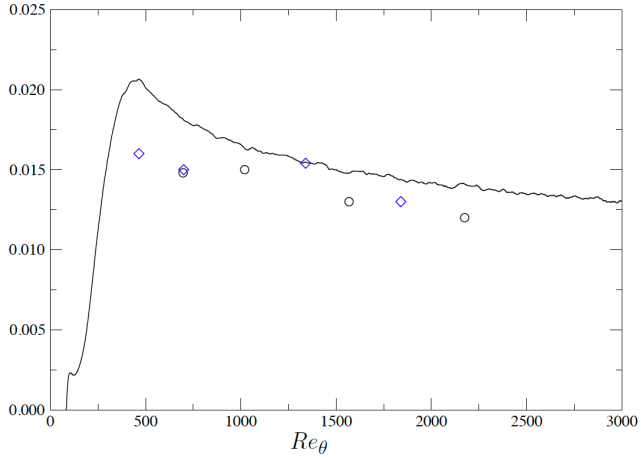

Figure 2. Local peak value of Reynolds stress component $u'^2_{x,rms}/U^2_\infty$ as a function of momentum thickness Reynolds number Re_θ in ZPGSFPBL. Subscript x refers to the boundary layer's streamwise direction. Solid line: DNS of ZPGSFPBL from laminar through bypass transition in the narrow sense to turbulent (Wu et al 2017); diamond: turbulent ZPGSFPBL experiments of Purtell et al (1981); circle: turbulent ZPGSFPBL experiment of Erm & Joubert (1991). It seems that in boundary layer there is a plausible overshoot of the peak Reynolds stress during the late stage of transition with respect to the level of turbulent ZPGSFPBL at the same Re_θ. The overshoot is nevertheless quite minor compared to the distinct sharp overshoot in pipe transition.

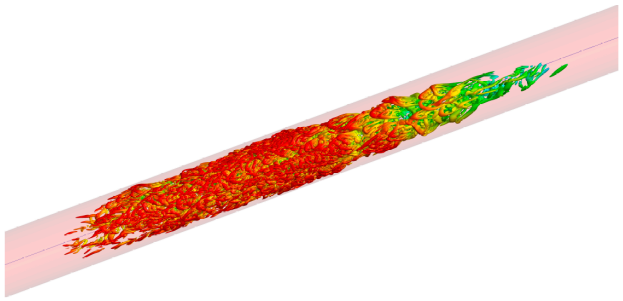

Figure 3. Turbulent spots in the transitional pipe flow at Re = 6500. It is evident that the near-wall region (red in color) is dominated by reverse hairpin vortices. Flow is from left to right.

Aside from the feasibility and validation study in Wu et al (2015) at $6000 < Re < 8000$, accuracy of the spatially-developing DNS approach is further demonstrated here at the low Reynolds number $Re = 2300$ by evaluating the friction factor $f = 8\tau_w/(\rho V^2)$ and centerline axial velocity u_z/V against their respective fully-developed laminar solution. τ_w is the wall shear stress. In Figure 4, the circumferentially averaged friction factor $\langle f \rangle$ at the instant $t = 500R/V$ is compared with the laminar solution $f = 64/Re$. It is seen from Figure 4 that the simulated friction factor remains almost exactly the same as the analytical laminar solution both before and after the passage of the packet of the two turbulent spots. Figure 4 also presents the centerline axial velocity u_z/V at $t = 500R/V$. In sharp contrast to previously published short-domain temporal pipe transition results, here, u_z/V is almost exactly 2.0 along the centerline except for the region perturbed by the packet of the two turbulent spots. The spatially-developing transition simulation approach, while far more accurate in comparison to the temporal approach with short-domain, is nevertheless quite expensive at the present $32768\times200\times256$ mesh, and it took one wall-clock year to advance $100{,}000\Delta t$ using 128 CPUs of Intel Xeon E5-2650.

Profiles of $\langle f \rangle(t, z)$ in Figure 4 suggest that the first splitting of the original parent occurs prior to $t = 500R/V$. The splitting process is documented in Figure 5 using the near-wall axial velocity profiles $u_z(t, z, r = 0.01)$ as a function of time. The profile at $t = 600R/V$ with two new minor secondary peaks implies perhaps the second splitting of the original parent spot and the first splitting of the child spot. The development from twin-peak at $t = 500R/V$ to quad-peak at $t = 600R/V$ is followed by an unclear complex pattern at $t = 700R/V$ and back to twin-peak at $t = 800R/V$. This may correspond to an unknown cycle. Obviously, the splitting events implied by these one-dimensional profiles are only suggestive and need to be confirmed and elucidated by three-dimensional visualization data. Figure 6 presents visualization of the parent spot and the decaying child spot at $t = 400R/V$ after the first splitting event using iso-surfaces of swirling strength. For conditional averaging purpose, each spot is subdivided into 9 equal-length segments. Within each segment streamwise homogeneity and circumferential homogeneity are assumed in the conditional averaging. Although not presented here, zonal conditionally averaged axial velocity component on the child spot sampled suggests that across a wide radial range there is a nearly constant speed lag between the middle-middle zone and the front--middle zone, suggesting that these spots are being subjected to sustained streamwise stretching. This indicates that sustained straining along the axial direction is perhaps the real mechanism behind the mysterious pipe flow spot splitting at low Reynolds number range.

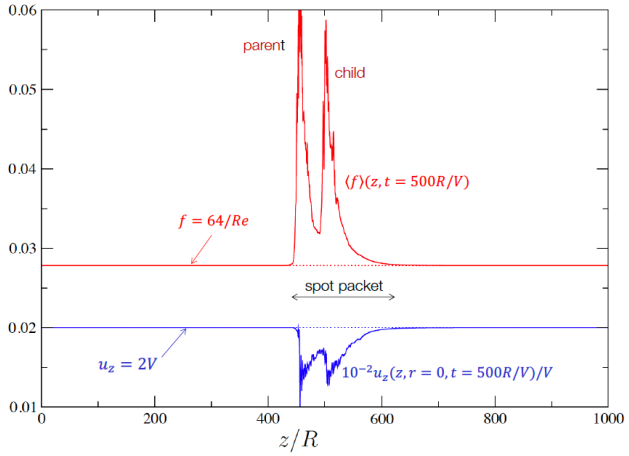

Figure 4. Demonstration of simulation accuracy of the present spatially-developing DNS of transitional pipe flow at $Re = 2300$. It is evident that, contrary to the temporal simulation results of existing DNS on transitional pipe flow, the present packet of turbulent spots is bounded from both upstream and downstream by fully-developed laminar flow.

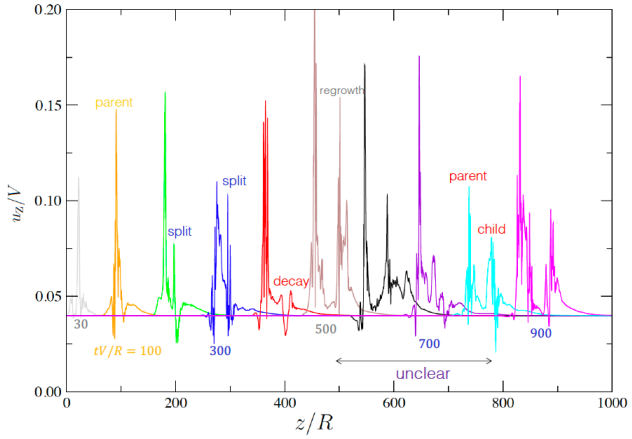

Figure 5. Variation of axial velocity along one near-wall axial line (r=0.99R) as packet of turbulent spots developing through the fully developed laminar pipe flow at $Re = 2300$. Variation of the magnitude of the secondary peaks at tV/R=300, 400 and 500 correspond to an initial decay and subsequent rejuvenation of the first child spot.

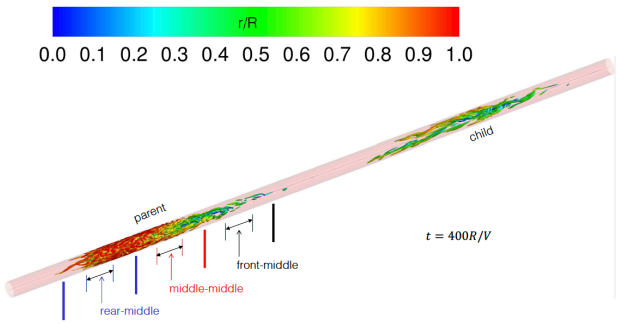

Figure 6. Visualization of the parent spot and the decaying child spot at tV/R=400 after the first splitting event using iso-surfaces of swirling strength. Re=2300. For conditional averaging purpose, each spot is subdivided into 9 equal-length segments.

REFERENCES

ACARLAR, M.M. & SMITH, C.R. 1987 A study of hairpin vortices in a laminar boundary layer. Part 2. Hairpin vortices generated by fluid injection. *J. Fluid Mech.* **175**, 43-83.

ADRIAN, R.J. 2007 Hairpin vortex organization in wall turbulence. *Phys Fluids* **19**, 041301.

AVILA, K., MOXEY, D., de LOZAR, A., AVILA, M., BARKLEY, D. & HOF, B. 2011 The onset of turbulence in pipe flow. *Science,* **333**, 192-196.

BANDYOPADHYAY, P.R. 1986 Aspects of the equilibrium puff in transitional pipe flow. *J. Fluid Mech*. **163**, 439–458.

BARKLEY, D., SONG, B., MUKUND, V., LEMOULT, G., AVILA, M. & HOF, B. 2015 The rise of fully turbulent flow. *Nature,* **526**, 550–553.

CHIN, C., OOI, A.S.H., MARUSIC, I. & BLACKBURN, H.M. 2010 The influence of pipe length on turbulence statistics computed from direct numerical simulation data. *Phys Fluids* **22**, 115107.

CHOI, H. & MOIN, P. 1990 On the space-time characteristics of wall-pressure fluctuations. *Phys Fluids A* **2**, 1450-1460.

DUGUET, Y., WILLIS, A.P. & KERSWELL, R.R. RR. 2010 Slug genesis in cylindrical pipe flow. *J. Fluid Mech*. **663**,180–208.

ERM, L.P. & JOUBERT, P.N. 1991 Low-Reynolds-number turbulent boundary layers. *J. Fluid Mech*. **230**, 1–44.

Hellström L.H.O. & Smits, A.J. 2017 Structure identification in pipe flow using proper orthogonal decomposition. *Philos T R Soc A* **375**, 20160086.

JIMÉNEZ, J., HOYAS, S., SIMENS, M.P. & MIZUNO, Y. 2010 Turbulent boundary layers and channels at moderate Reynolds numbers. *J. Fluid Mech*. **657**, 335–360.

KLEISER, L. & ZANG, T.A. 1991 Numerical simulation of transition in wall-bounded shear flows. *Annu Rev Fluid Mech.* **23**, 495-537.

LEE, J.H. & SUNG, H.J. 2011a Direct numerical simulation of a turbulent boundary layer up to $Re_\theta = 2500$. *Int. J. Heat Fluid Flow* **32**, 1-10.

LEE, J.H. & SUNG, H.J. 2011b Very-large-scale motions in a turbulent boundary layer. *J. Fluid Mech*. **673**, 80-120.

LEONARD, A. 1983 Numerical simulation of turbulent flows. *NACA TM* 84320.

LINDGREN, E.R. 1953 Some aspects of the change between laminar and turbulent flow of liquids in cylindrical tubes. *ARKIV FYSIK* **3**, 293-308.

LINDGREN, E.R. 1959a Liquid flow in tubes I. The transition process under highly disturbed entrance flow conditions. *ARKIV FYSIK* **15**, 97-119.

LINDGREN, E.R. 1959b Liquid flow in tubes II. The transition process under less disturbed inlet flow conditions. *ARKIV FYSIK* **15**, 503-519.

LINDGREN, E.R. 1959c Liquid flow in tubes III. Characteristic data of the transition process. *ARKIV FYSIK* **16**, 101-112.

MOIN, P. & KIM, J. 1985 The structure of the vorticity field in turbulent channel flow. Part 1. Analysis of instantaneous fields and statistical correlations. *J Fluid Mech.* **608**, 81-112.

MOXEY, D. & BARKLEY, D. 2010 Distinct large-scale turbulent-laminar states in transitional pipe flow. *Proc Nat Acad Sci U.S.A.* **107**, 8091-8096.

MULLIN, T. 2011 Experimental studies of transition to turbulence in a pipe. *Ann Rev Fluid Mech*. **43**, 1-24.

PEIXINHO, J. & MULLIN, T. 2007 Finite-amplitude thresholds for transition in pipe flow. *J Fluid Mech.* **582**, 169-178.

PIERCE, C.D. & MOIN, P. 2001 Progress variable approach for large-eddy simulation of turbulent combustion. *Mech. Eng. Dept. Rep.* TF-80, Stanford University.

PIERCE, C.D. & MOIN, P. 2004 Progress variable approach for large-eddy simulation of non-premixed turbulent combustion. *J Fluid Mech*. **504**, 73-97.

PRIYMAK, V.G. & MIYAZAKI, T. 2004 Direct numerical simulation of equilibrium spatially localized structures in pipe flow. *Phys Fluids* **16**, 4221.

PURTELL, L.P., KLEBANOFF, P.S. & BUCKLEY, F.T. 1981 Turbulent boundary layer at low Reynolds number. *Phys Fluids* **24**, 802-811.

REYNOLDS, O. 1883 An experimental investigation of the circumstances which determine whether the motion of water shall

be direct or sinuous, and of the law of resistance in parallel channels. *Philos T R Soc A* **174**, 935–982.

ROGERS, M.M. & MOIN, P. 1987 The structure of the vorticity field in homogeneous turbulent flows. *J Fluid Mech.* **176**, 33-66.

SAU, R. & MAHESH, K. 2008 Dynamics and mixing of vortex rings in crossflow. *J Fluid Mech.* **604**, 389-409.

SAYADI, T., HAMMAN, C.W. & MOIN, P. 2013 Direct numerical simulation of complete H-type and K-type transitions with implications for the dynamics of turbulent boundary layers. *J Fluid Mech.* **724**, 480-509.

SCHLATTER, P. & ÖRLÜ, R. 2010 Assessment of direct numerical simulation data of turbulent boundary layers. *J. Fluid Mech*. **659**, 116-126.

SCHLATTER, P. & ÖRLÜ, R. 2012. Turbulent boundary layers at moderate Reynolds numbers: inflow length and tripping effects. *J. Fluid Mech*. **710**:5-34

SCHUBAUER, G.B. & SKRAMSTAD, H.K. 1947 Laminar boundary-layer oscillations and stability of laminar flow. *J. Aeronau. Sci*., **14**, 88-97.

SCHUBAUER, G.B. & KLEBANOFF, P.S. 1955 Contributions on the mechanics of boundary layer transition. *NACA Technical Note* 3489.

SHAN, H., MA, B., ZHANG, Z. & NIEUWSTADT, F.T.M. 1999 Direct numerical simulation of a puff and a slug in transitional cylindrical pipe flow. *J. Fluid Mech.*, **387**, 39-60

SHIMIZU, M. & KIDA, S. 2009 A driving mechanism of a turbulent puff in pipe flow. *Fluid Dyn. Res*. **41**, 045501.

VANDERWEL, C. & TAVOULARIS, S. 2011 Coherent structures in uniformly sheared turbulent flow. *J. Fluid Mech.* **689**, 434-464.

WILLIS, A.P. & KERSWELL, R.R. 2007 Critical behavior in the relaminarization of localized turbulence in pipe flow. *Phy. Rev. Lett.,* **98**, 014501.

WU, X. & MOIN, P. 2008 A direct numerical simulation study on the mean velocity characteristics in turbulent pipe flow. *J. Fluid Mech.*, **608**, 81-112.

WU, X. & MOIN, P. 2009 Direct numerical simulation of turbulence in a nominally zero-pressure-gradient flat-plate boundary layer. *J. Fluid Mech.*, **630**, 5-41.

WU, X. & MOIN, P. 2010 Transitional and turbulent boundary layer with heat transfer. *Phys Fluids* **22**, 85-105.

WU, X. & MOIN, P., ADRIAN, R.J. & BALTZER, J.R. 2015 Osborne Reynolds pipe flow: Direct simulation from laminar through gradual transition to fully developed turbulence. *Proc. Nat. Acad. Sci. USA*. **112**, 7920-7924.

WU, X. & MOIN, P., WALLACE, J.M., SKARDA, J., ADRIÁN, LOZANO-DURÁN & HICKEY, J-P. 2017. Transitional-turbulent spots and turbulent-turbulent spots in boundary layers. *Proc. Nat. Acad. Sci. USA*. **114**, E5292-E5299.

WYGNANSKI, I.J. & CHAMPAGNE, F.H. 1973. On transition in a pipe. Part 1. The origin of puffs and slugs and the flow in a turbulent slug. *J. Fluid Mech.* **59**, 281-335.